

# Stratiform precipitation production over sub-Saharan Africa and the tropical East Atlantic as observed by TRMM

By COURTNEY SCHUMACHER<sup>1\*</sup> and ROBERT A. HOUZE, JR.<sup>2</sup>

<sup>1</sup>*Department of Atmospheric Sciences, Texas A&M University, USA*

<sup>2</sup>*Department of Atmospheric Sciences, University of Washington, USA*

(Received 8 June 2005; revised 30 May 2006)

## SUMMARY

Convective systems over sub-Saharan Africa and the tropical East Atlantic have distinct geographical and seasonal variations in convective intensity and stratiform precipitation production as observed by the Tropical Rainfall Measuring Mission (TRMM) Precipitation Radar. Over the East Atlantic, convective rain rates are lower and the percentage of total rain that is stratiform is higher compared to over West Africa. In addition, the East Atlantic has more shallow precipitating convection and less non-precipitating anvil than sub-Saharan Africa. During the monsoon season, convective rain rates and the percentage of area covered by anvil decrease while the stratiform rain fraction and number of shallow convective cells increase in both regions compared to the pre-monsoon season. These observations suggest that convective sustainability, i.e. the ability of a region to continually support convection, helps determine whether a robust stratiform rain area or non-precipitating anvil forms.

In addition to convective sustainability, wind shear and the Saharan Air Layer appear to play important roles in the formation and extent of the stratiform components of convective cloud systems. Strong winds associated with the African Easterly Jet and dry intrusions from the Sahara Desert may increase sublimation and evaporation at mid levels, resulting in less stratiform rain. Strong upper-level shear associated with the African Easterly Jet may further hinder stratiform rain production by displacing hydrometeors that form in the convective cells beyond the area of mesoscale rain formation. When the upper-level Tropical Easterly Jet strengthens during the monsoon season, upper-level shear is reduced dramatically and stratiform rain areas form in preference to non-raining anvil.

**KEYWORDS:** Mesoscale organization Radar observations Tropical convection West Africa

## 1. INTRODUCTION

Satellite studies of sub-Saharan Africa and the adjacent equatorial Atlantic Ocean are beginning to provide a new perspective on the nature of mesoscale convective systems (MCSs) affecting these regions. Sub-Saharan MCSs are faster and shorter lived than their counterparts over the East Atlantic (Hodges and Thorncroft 1997) and have significantly stronger 85 GHz ice-scattering signatures (Mohr *et al.* 1999; Toracinta and Zipser 2001). Lightning-producing clouds are seven times more likely to occur over sub-Saharan Africa than over the Atlantic, while cell flash rates only vary by a factor of two (Boccippio *et al.* 2000). Average conditional rain rates are much stronger over sub-Saharan Africa compared to the East Atlantic, and a smaller fraction of the total rain is stratiform (Schumacher and Houze 2003a). Also, West African precipitation peaks between late afternoon and midnight, while eastern Atlantic precipitation peaks during the day (McGarry and Reed 1978; Laing and Fritsch 1993; Yang and Slingo 2001; Nesbitt and Zipser 2003). These distinct differences call into question the factors that affect MCSs over sub-Saharan Africa and the tropical East Atlantic.

MCSs over West Africa often take the form of rapidly moving squall lines (Hamilton and Archbold 1945; Eldridge 1957; Fortune 1980; Sommeria and Testud 1984; Chong *et al.* 1987; Roux 1988; Chong and Hauser 1989). However, satellite census shows that two distinct types of MCS exist, rapidly moving squall lines and slower moving non-squall MCSs, and that both types of MCS occur in relation to synoptic-scale

\* Corresponding author: Department of Atmospheric Sciences, Texas A&M University, 3150 TAMU, College Station, TX 77843, USA. e-mail: courtney@ariel.met.tamu.edu

easterly waves and/or convergence in the low-level monsoon trough (Aspliden *et al.* 1976; Payne and McGarry 1977; Martin and Schreiner 1981; Houze and Betts 1981). Rowell and Milford (1993) demonstrated that the squall line disturbances occur when a potentially unstable low-level moisture source is overlain by dry desert air and vertical shear exists beneath the African Easterly Jet (AEJ). In addition, stronger low-level westerlies and the presence of mountains promote squall-line formation and longevity. Rowell and Milford's results were based on one month of satellite infrared (IR) data. Based on eight years of IR data, Hodges and Thorncroft (1997) more generally show that these conditions are conducive to the genesis and longevity of the broader spectrum of MCSs.

More recently, other studies have suggested links between the AEJ and long-term Sahelian precipitation (e.g. Cook 1999; Diedhiou *et al.* 1999; Grist and Nicholson 2001), but less attention has been focused on the varying nature of the convective systems producing the precipitation. The majority of rain produced in West Africa comes from MCSs (Lebel *et al.* 2003), so it is important to understand these systems, including the stratiform precipitation component. In addition, little attention has been paid to convective systems over the East Atlantic since the Global Atmospheric Research Programme's Atlantic Tropical Experiment (GATE) in 1974 (Houze and Betts 1981). MCSs and their associated stratiform precipitation components are also important to total East Atlantic rainfall, and the connection between MCSs over sub-Saharan Africa and the East Atlantic is relevant to studies of Atlantic tropical cyclone activity (Carlson 1969a,b; Landsea and Gray 1992; Thorncroft and Hodges 2001).

This study focuses on differences in the convective precipitation features and large-scale environmental factors that accompany variations in stratiform rain production over West Africa and the tropical East Atlantic. We analyse observations from the Tropical Rainfall Measuring Mission (TRMM) satellite and National Centers for Environmental Prediction (NCEP) reanalysis fields of relative humidity and wind before and during the full cycle of the African monsoon to understand what drives the observed temporal and geographical variations in the percentage of total rain that is stratiform. Analysis of these datasets shows that the ability of precipitating convective cloud systems over sub-Saharan Africa and the tropical East Atlantic to support convective systems with large stratiform rain areas is affected by the following factors. First, large-scale wind shear and environmental humidity are important. In addition, the data indicate that the ability of the environment to support convection via a long-lasting widespread warm moist boundary layer is critical. This latter factor has been referred to as convective sustainability by Yuter and Houze (1998) and Houze (2004).

## 2. TRMM PRECIPITATION RADAR DATA

This study uses observations from 1998 to 2003 from the Precipitation Radar (PR) onboard the TRMM satellite. From January 1998 to August 2001, the TRMM satellite operated at an altitude of 350 km, which gave the PR a swath width of 215 km and a horizontal footprint of 4.3 km at nadir. The satellite was boosted to 402.5 km in August 2001 to conserve fuel, after which the PR had a swath width of 245 km and a footprint of 5 km at nadir. Shimizu *et al.* (2003) have shown that besides the expected post-boost degradation in sensitivity of 1.2 dB, there were no other significant discontinuities in PR observations at the time of the boost.

The PR operates at  $K_u$  band (2.17 cm wavelength) with a sensitivity  $\sim 17$  dBZ pre-boost and 18 dBZ post-boost, which corresponds to a rain rate of approximately 0.4–0.5 mm h<sup>-1</sup>. The PR can detect some reflectivities down to  $\sim 14$  dBZ, but not in

proportion to actual occurrence. In addition, the TRMM satellite has a precessing orbit so that it samples the full diurnal cycle, and the vertical resolution of the PR is 250 m at nadir. Further details on the PR and the TRMM satellite can be found in Kummerow *et al.* (1998) and Kozi *et al.* (2001).

The radar echo observed by the PR is subdivided into convective and stratiform elements in TRMM product 2A23 (Awaka *et al.* 1997). The convective classification refers to areas of young, active convection, where stronger vertical air motions predominate and precipitation particles increase in mass through coalescence and/or riming (Houze 1993, 1997). Microphysical growth processes can occur throughout the depth of the troposphere in convective clouds. The stratiform classification represents areas of less active convection, where weaker vertical air motions predominate and precipitation particles increase in mass primarily through vapour deposition above the 0 °C level and decrease in mass through evaporation below the 0 °C level. The 2A23 algorithm determines whether the echo is convective or stratiform by examining the vertical profile of reflectivity (from which the bright band, echo-top height, and maximum reflectivity in the vertical profile are identified) and the horizontal variability of the echo. Within the Version 5 2A23 algorithm, the convective and stratiform echo categories are further subdivided into 18 subtypes (Schumacher and Houze 2003b). This study uses the subtypes identified within the Version 5 2A23 algorithm to define four general echo types:

*Shallow isolated* echoes (types 15, 26–29). Shallow isolated echoes are typically only a few kilometres in width and height and often occur over the ocean in low rain regions (Schumacher and Houze 2003b). Echo is designated shallow isolated if the echo-top height is at least 1 km beneath the 0 °C level (located at about 5 km altitude in the tropics) and the cell is not attached to non-shallow echo. Figure 1(a) shows a mix of PR-observed shallow isolated cells and slightly deeper, but still relatively weak, single-cell cumulonimbus clouds off the coast of West Africa.

*Convective* echoes (types 20–25). Convective echoes in the tropics exhibit a spectrum of sizes (Houze and Cheng 1977; Cetrone and Houze 2005). Figure 1(b) shows an example of weak to moderate convective cells over the East Atlantic that resemble the cells illustrated in Fig. 1(a); however, the cells in Fig. 1(b) are a bit deeper and tend to cluster together in small groups. Examples of two very intense, deep convective echoes seen by the PR over West Africa are shown in Fig. 1(d). Deep convective echoes consist of vertically oriented echo cores, typically ~10 km in width, and they may extend to heights of 17 km or more. The maximum reflectivity values often reach 50 dBZ or more, but in the tropics the maximum reflectivity values are usually found below the 0 °C level.

*Stratiform* echoes (types 10–14). Stratiform precipitation is identified in the 2A23 algorithm as echo from precipitation reaching the surface and exhibiting a bright band (i.e. a maximum of reflectivity in the melting layer) and/or with relatively little horizontal variability in echo intensity. Stratiform radar echoes exhibit a range of structures. At one extreme, the formation of a bright band and a more stratiform structure can occur in the late stages of the convective life cycle, when convective cells in close proximity decay more or less simultaneously (Houze 1997). This decay is beginning to occur in Fig. 1(b), while a more mature example of this type of stratiform echo is shown in Fig. 1(c). In this scenario, the precipitation pattern is generally light and patchy in the horizontal, but the vertical structure of the echo indicates the presence of a weak bright band. At the other end of the development spectrum of stratiform precipitation structures, large areas of moderately intense stratiform precipitation form in association with robust mesoscale convective systems. An example of a larger non-squall line system was described for the eastern tropical Atlantic off the coast of Africa by Leary

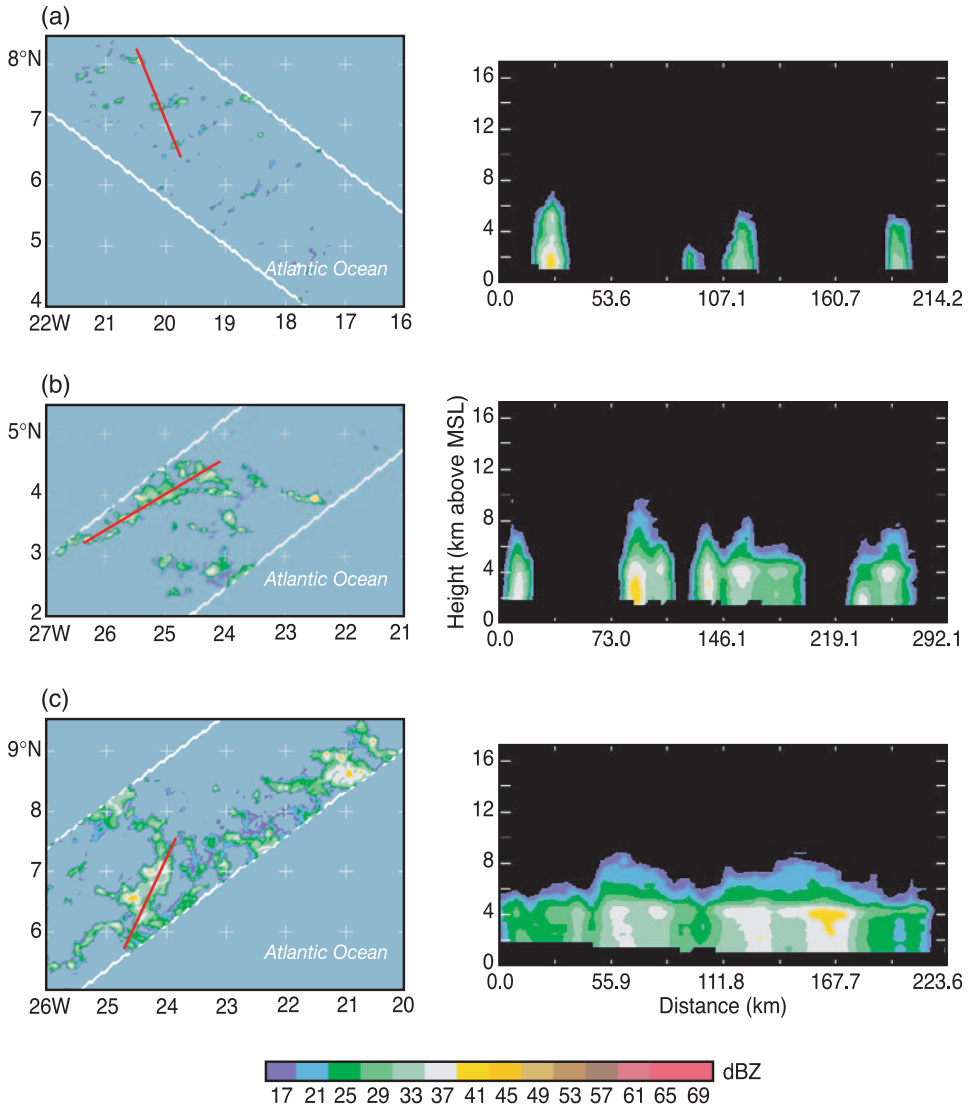


Figure 1. PR-observed convective systems over the East Atlantic and West Africa during 2004 based on TRMM product 2A25 data. Cases represent (a) a mix of shallow isolated echo and slightly deeper convective echo (30 June—Orbit 37750), (b) weak to moderate convective echo (1 June—Orbit 37301), (c) weakly organized stratiform echo (22 June—Orbit 37637), (d) and (e) deep convective echo with an extensive anvil (14 June—Orbit 37514) and (f) a squall line with an extensive stratiform area (19 May—Orbit 37108). Horizontal cross-sections are at 2 km altitude and vertical cross-sections are taken along the red line from west to east. The colour scale indicates reflectivity in dBZ. Each case is further described in the text.

and Houze (1979). The system was similar in appearance to Fig. 1(c), but somewhat broader and deeper. Rapidly propagating squall-line MCSs of the leading-line/trailing stratiform type represent another type of convective system with a large stratiform area (Zipser 1969, 1977; Houze 1977, 2004). An example of a leading-line/trailing stratiform squall line is shown in Fig. 1(f). This type of stratiform precipitation can be formed from ice particles advected from the upper regions of the squall-line convective cells (Biggerstaff and Houze 1993) or by the discrete propagation process in which a new



Figure 1. Continued.

convective line forms ahead of the current line and subsequently the current line decays and turns stratiform while the new line takes over as the leading line (see Houze 2004). The discrete propagation mechanism of stratiform precipitation formation is similar to the formation of the non-squall line stratiform areas of the type in Fig. 1(c).

*Anvil* echoes (types 30–31, identified as ‘other’ in the algorithm). These are echoes aloft that do not reach down to the Earth’s surface. These echoes may be attached to convective or stratiform echoes of the types described above. Deep convective systems over West Africa frequently develop anvil echoes (e.g. Fig. 1(e)). Since the sensitivity of the PR is only about 17 dBZ (18 dBZ post-boost), hydrometeors probably exist at levels both above and below the anvils seen in the PR data. However, the PR anvil certainly represents the substantive core of the anvil layer aloft. This terminology, which has been adopted by the TRMM community for describing PR echoes, is somewhat different from that in some past studies that have used the term anvil precipitation to describe what we define herein as stratiform echo (see above).

In the remainder of this paper, we compile statistics of these four echo types, first across the tropics and then over West Africa and the adjoining eastern tropical Atlantic Ocean. Our analysis is based on histograms compiled from the Version 5 orbital data mined by the TRMM Science Data and Information System (TSDIS). For each rain type, attenuation-corrected reflectivity observations from TRMM product 2A25 (Iguchi *et al.* 2000) were categorized by height (500 m increments from 1 to 15 km) and reflectivity (2 dBZ bins from 14 to 60 dBZ) at  $2.5^\circ \times 2.5^\circ$  resolution in daily files. The resulting histograms have 28 latitude bins, 144 longitude bins, 28 height bins and 23 reflectivity bins. They can be added together to form monthly, seasonal or annual histograms. These histograms offer higher resolution in time and space and more flexibility in rain type compared to the monthly gridded histograms in TRMM product 3A25.

### 3. TROPICS-WIDE STATISTICS OF REFLECTIVITY PROFILES

Figure 2 shows the vertical distribution of the tropics-wide ( $20^\circ\text{N}$ – $20^\circ\text{S}$ ) reflectivity for the four echo types described in section 2. Each line represents a 10% quantile (from 10 to 90%) of echo occurrence with height. Height levels with less than 0.5% of the total count are not plotted. In the stratiform profiles (Fig. 2(a)) the bright band is evident in the 4–5 km layer, which lies just below the climatological  $0^\circ\text{C}$  isotherm in the tropics. Beneath the bright band, reflectivity remains fairly constant in magnitude down to the surface. The median near-surface reflectivity (thick, solid line) is 25 dBZ ( $\sim 1 \text{ mm h}^{-1}$ ). Above the bright band, reflectivities are generally  $< 25$  dBZ and the quantiles are tightly packed. These features suggest a narrow distribution of weak vertical velocities and relatively homogeneous ice growth processes (i.e. diffusional growth in upper levels of the stratiform rain region). To place the examples from the previous section in perspective—the echo intensities in the aging convective cells in Fig. 1(b) are consistent with median tropics-wide stratiform reflectivities, while the more robust stratiform areas in Figs. 1(c) and (f) fall within the 90% quantile.

In the convective profiles (Fig. 2(b)), there is a much broader distribution of echo intensity above the  $0^\circ\text{C}$  level along with larger reflectivity values. These features are indicative of stronger and more varied vertical velocities and more heterogeneous hydrometeor growth processes (e.g. riming in addition to diffusional growth). Beneath the  $0^\circ\text{C}$  level, the convective reflectivity profiles tend to increase toward the surface and the median near-surface reflectivity is 34 dBZ ( $\sim 6 \text{ mm h}^{-1}$ ), significantly stronger than the stratiform median value. The intense convective towers in Fig. 1(d) fall within the 90% quantile compared to tropics-wide convective reflectivities, while the weaker convection over the East Atlantic in Figs. 1(a) and (b) represent median or lower quantiles. The anvil profiles (Fig. 2(c)) generally show weaker reflectivity aloft with very little near-surface rain (most likely virga)\*. The anvil in Fig. 1(e) ranges in height from 4 to 10 km, which is consistent with the PR tropics-wide anvil reflectivity profiles. The shallow isolated profiles (Fig. 2(d)) do not extend above the freezing level, indicating the predominance of warm rain processes (Schumacher and Houze 2003b). Reflectivity increases toward the surface in the shallow cells, but near-surface reflectivity is relatively weak.

The profiles in Fig. 2 do not extend all the way to the surface because the PR cannot detect rain directly above the ocean or land as a result of contamination by

\* Schumacher and Houze (2000) showed that the PR misses  $< 3\%$  of the total surface rain observed by the Kwajalein ground radar. Therefore, the anvil category would at most account for a few percent of the total rain. This value is likely much less since undetected stratiform and convective rain account for some of the missing amount.

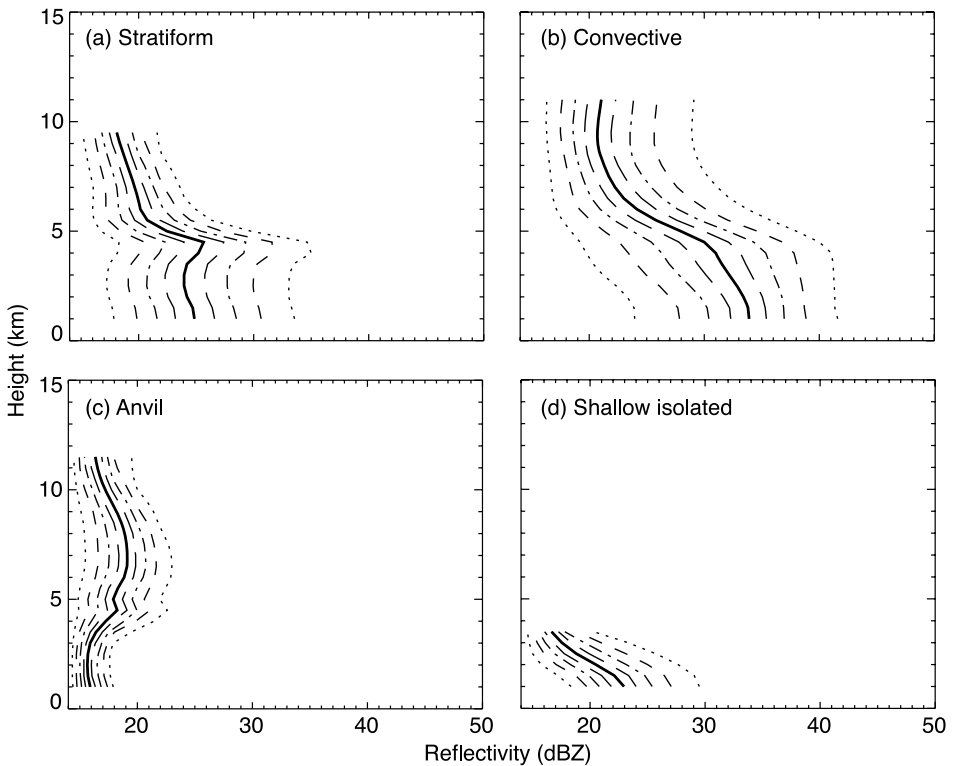


Figure 2. Vertical distributions of reflectivity for stratiform, convective, anvil and shallow rain types as defined by the Version 5 TRMM 2A23 algorithm. The profiles include all PR observations between 20°N and 20°S from 1998 to 2003. Each line represents a 10% quantile from 10 to 90%; the median profile is the solid, thick line.

surface return. The lowest level free from surface clutter is  $\sim 1$  km above the surface at nadir and  $\sim 2$  km above the surface at the antenna scan edge. Therefore, to determine rain statistics we use 2 km PR observations. Low-level reflectivity measurements are also subject to attenuation due to the operating wavelength of the PR. Comparisons with non-attenuated ground radar observations suggest that the PR 2A25 algorithm does well at correcting for attenuation at altitudes near 2 km (Bolen and Chandrasekar 2000; Schumacher and Houze 2000).

As in Schumacher and Houze (2003a), binned orbital 2 km reflectivity is converted to rain rate using the TRMM version 5 convective and stratiform near-surface initial reflectivity–rain rate ( $Z$ – $R$ ) relations ( $Z = 148 R^{1.55}$  and  $Z = 276 R^{1.49}$ , respectively). The average convective and stratiform rain rate in each grid box is then multiplied by the probability of rain for each rain type and the number of hours in the time period of interest (typically a month) to obtain the convective and stratiform rain amounts. There is debate in the literature as to whether it is more appropriate to use a single  $Z$ – $R$  relation or separate convective and stratiform  $Z$ – $R$  relations. We use separate relations since that is the TRMM PR convention; however, the reader should note that  $Z$ – $R$  relation variations can bias the convective and stratiform rain statistics, but that the bias should not affect the comparative results in the following section. Further discussion on the sensitivity of PR rain statistics to  $Z$ – $R$  variations can be found in the appendix of Schumacher and Houze (2003a).

#### 4. REGIONAL PRECIPITATION CLIMATOLOGY ASSOCIATED WITH RADAR ECHO TYPES

The regions of interest in this study are the East Atlantic ( $5^{\circ}\text{S}$ – $17.5^{\circ}\text{N}$ ,  $30$ – $17.5^{\circ}\text{W}$ ) and sub-Saharan West Africa ( $5$ – $17.5^{\circ}\text{N}$ ,  $17.5^{\circ}\text{W}$ – $10^{\circ}\text{E}$ ) and are indicated by the boxes in Fig. 3. We analyse TRMM PR observations over these regions for March, April and May (MAM) and June, July and August (JJA) (the pre-monsoon and monsoon, respectively) for 1998–2003. Figure 3 shows maps of the total rain, the percentage of total rain that is stratiform, and the conditional convective rain rates for each region and season. During MAM, the main area of precipitation lies along or just north of the equator with most of the West African rain occurring on the Gulf of Guinea coast ( $5^{\circ}\text{N}$ ,  $10^{\circ}\text{W}$ – $10^{\circ}\text{E}$ ; Fig. 3(a)). The average stratiform rain fraction (i.e. the total stratiform rain amount divided by the total rain amount in each box multiplied by 100) is 40% over the East Atlantic and 23% over West Africa (Fig. 3(b)). (The annual average over the whole tropics is 40%; Schumacher and Houze 2003a.) Convective rain rates are significantly stronger over West Africa, averaging  $14\text{ mm h}^{-1}$  compared to  $7\text{ mm h}^{-1}$  over the East Atlantic (Fig. 3(c)). Stratiform rain rates (not shown) are only slightly stronger over West Africa than over the East Atlantic, averaging  $1.9\text{ mm h}^{-1}$  and  $1.5\text{ mm h}^{-1}$ , respectively. Figure 3(d) further indicates that there is a lightning maximum over the Congo basin centred near the equator and  $20^{\circ}\text{E}$  and a secondary maximum over sub-Saharan Africa\*. Lightning is rare over the East Atlantic.

In JJA, the main precipitation band shifts northward to  $\sim 10^{\circ}\text{N}$  (Fig. 3(e)). The East Atlantic receives the same amount of rain each season ( $\sim 85\text{ mm mo}^{-1}$  averaged over the designated box), while the average stratiform rain fraction increases to 50% (Fig. 3(f)). The average rain accumulation more than doubles over West Africa during the monsoon season (from  $80$  to  $170\text{ mm mo}^{-1}$ ) and the average stratiform rain fraction increases to 35%. Note that a region of low stratiform rain fraction remains confined to the edge of the Sahara Desert. This pattern suggests that the increase in stratiform rain fraction over West Africa is more likely attributable to the offshore marine regime moving inland as opposed to a local increase over the land. The West African seasonal variation in stratiform rain fraction is consistent with a separate analysis of PR-observed rainfall done by Sealy *et al.* (2003). There is little change in the East Atlantic convective and stratiform rain rates between seasons, but the West African convective rain rate decreases slightly (Fig. 3(g)) and the stratiform rain rate increases slightly during the monsoon. The lightning maxima over Africa shift northward with the regions of high precipitation (Fig. 3(h)).

The mountainous regions in the eastern part of sub-Saharan Africa play an important role in the initiation and maintenance of large MCSs (Maddox 1980; Laing and Fritsch 1993; Hodges and Thorncroft 1997). There are only a few regions above 600 m in elevation in West Africa, which are indicated by the black shading in Fig. 3, so topography likely plays a lesser role in the organization and lifetime of MCSs in the western portion of sub-Saharan Africa. However, during JJA Fig. 3(e) shows that higher rain amounts (and to a lesser extent higher stratiform rain fractions) tend to occur on the western side of mountainous regions. This geographical variation is likely a result of orographic enhancement induced by the monsoon south-westerlies.

\* The v0.1 gridded time series satellite lightning data were produced by the NASA LIS/OTD (Lightning Imaging Sensor/Optical Transient Detector) Science Team (Principal Investigator, Hugh J. Christian, NASA/Marshall Space Flight Center) and are available from the Global Hydrology Resource Center (ghrc.msfc.nasa.gov). The lightning data represent seasonal averages from 1998 to 2001.

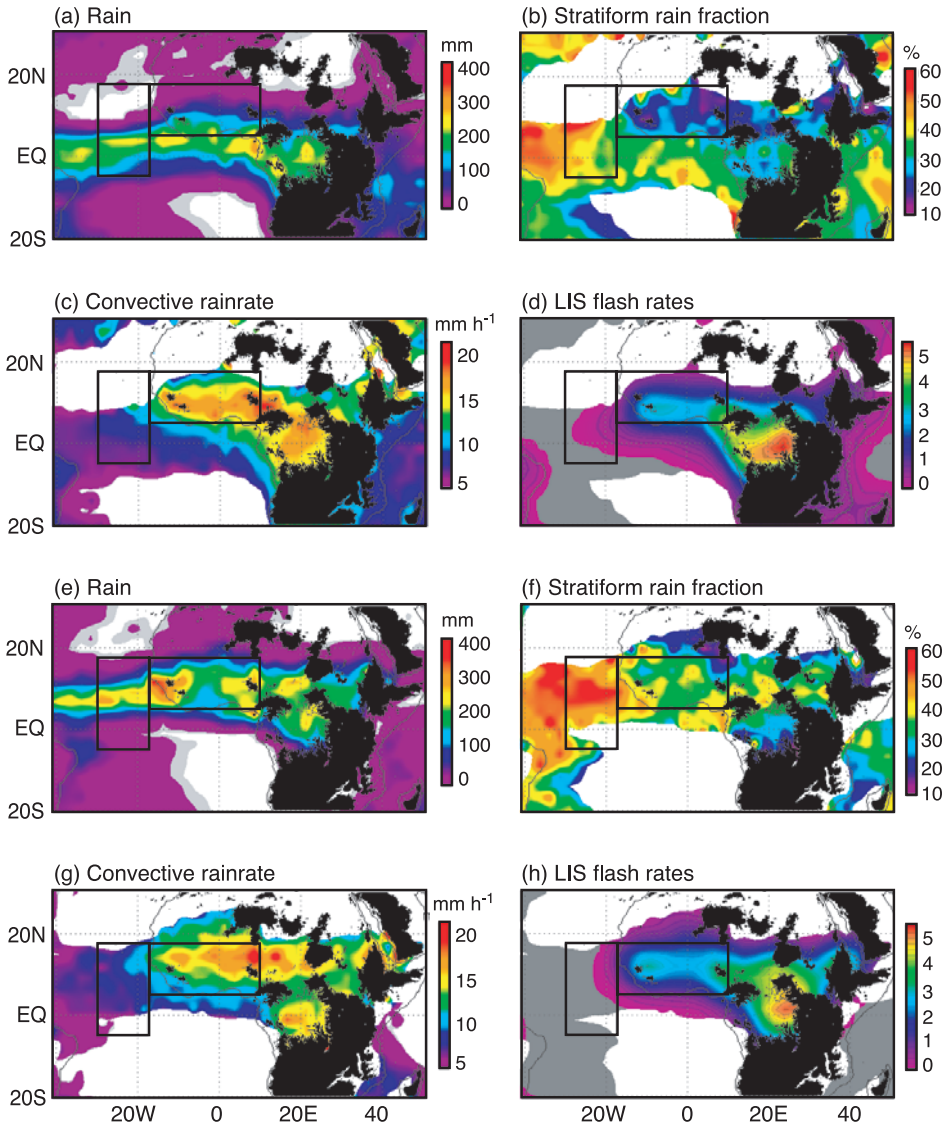


Figure 3. PR-observed mean monthly rain amount, stratiform rain fraction, and conditional convective rain rate at 2 km and LIS-observed lightning flash rates for (a–d) MAM and (e–h) JJA between 1998 and 2003. Data resolution is  $2.5^\circ$  and a rain threshold of  $10 \text{ mm mo}^{-1}$  is applied to all maps except rain accumulation. The regions of interest in this study are delineated by boxes. Black shading indicates orography greater than 600 m.

##### 5. REFLECTIVITY PROFILES BY GEOGRAPHICAL REGION AND SEASON

Figure 4 shows convective and stratiform reflectivity distributions with height for the East Atlantic and West Africa during JJA. Immediately obvious is the major difference between the convective profiles of the East Atlantic and West Africa (Figs. 4(a) and 4(b)). The East Atlantic profiles do not have a very large spread above the  $0^\circ\text{C}$  level; there are almost no observations of reflectivity  $>30 \text{ dBZ}$  above 5 km and data become sparse above 10 km. The West African profiles have a larger spread and are much more robust above the  $0^\circ\text{C}$  level. Adequate observations (i.e. at least 0.5% of the

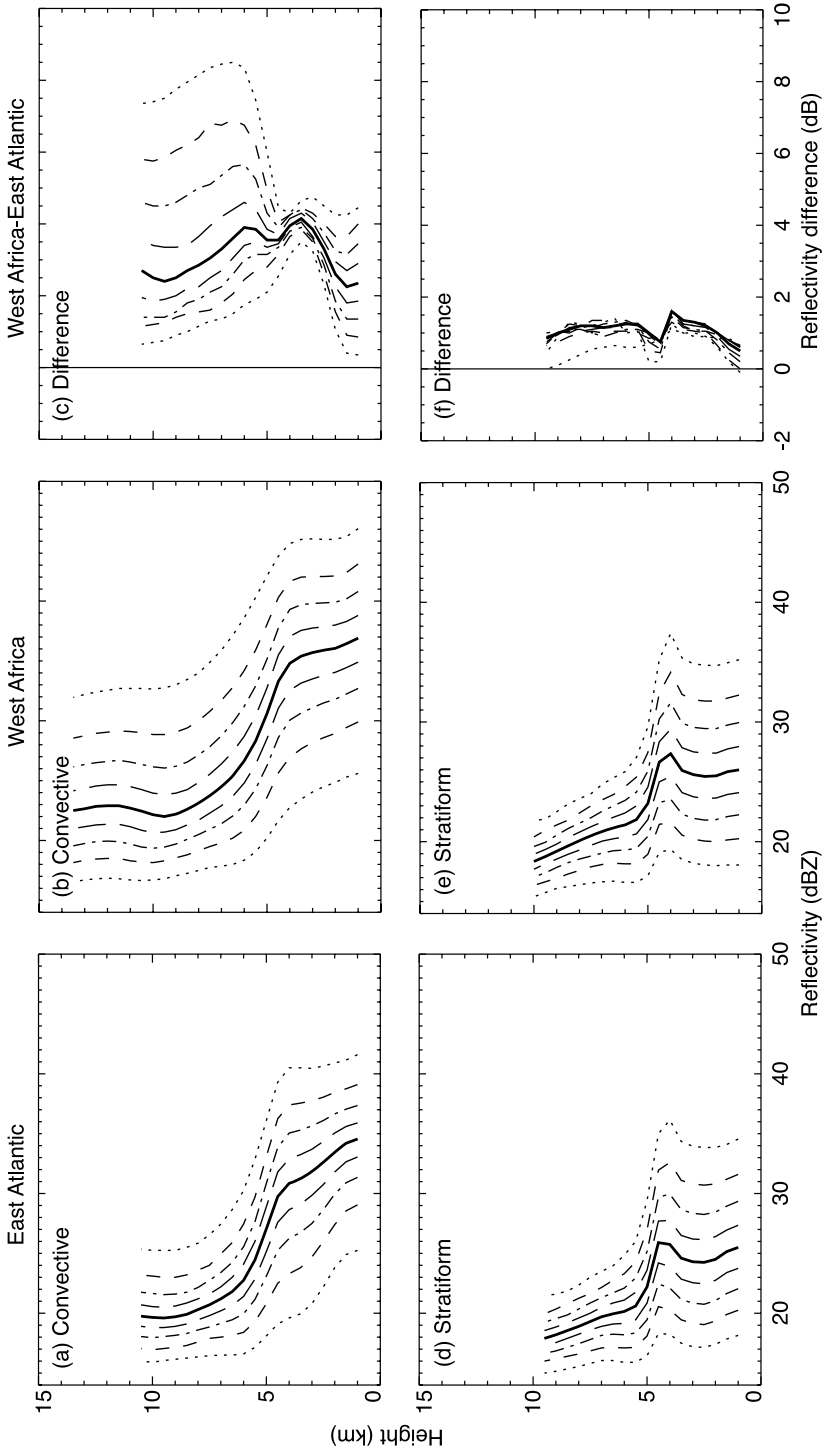


Figure 4. Vertical distributions of reflectivity for convective and stratiform precipitation over the East Atlantic and West Africa for JJA 1998–2003 following the plotting convention in Fig. 2. In addition, the difference between the West Africa and East Atlantic profiles is plotted for convective and stratiform reflectivities.

total observations) occur up to 13.5 km and there is a significantly larger population of observations of reflectivity  $>30$  dBZ above 5 km, suggesting graupel production. Geerts and Dejene (2005) also found evidence of large hydrometeor loading in PR-observed reflectivity profiles over West Africa. The right-hand panel (Fig. 4(c)) explicitly shows the difference in the convective reflectivity quantiles between the two regions. The reflectivity over West Africa is 1–8 dB greater at upper levels and 0.5–4.5 dB greater at lower levels, suggesting stronger and more varied vertical velocities within the deep convective clouds over sub-Saharan Africa, especially in the higher-altitude glaciated regions of the clouds.

The stratiform profiles are much more similar between the two regions (Figs. 4(d) and 4(e)). Both sets of profiles have bright bands strongly evident between 4 and 5 km and the profiles change little beneath the bright band to the surface. Profiles above the bright band are closely packed, indicating homogeneous ice microphysical processes. The difference plot (Fig. 4(f)) shows that West African stratiform areas have reflectivities that are about 1 dB stronger throughout the depth of the cloud system and slightly lower bright-band peaks. The decrease in difference at the surface may be attributed to stronger evaporation over the West African land surface, in agreement with the PR profile analysis performed by Hirose and Nakamura (2004). The similarity of the stratiform reflectivity distributions suggests that there are no major differences in the thermodynamics and kinematics of the stratiform precipitation areas over the East Atlantic and sub-Saharan Africa. Houze (1989) noted that from region to region, stratiform vertical motion profiles varied only slightly, while convective area profiles exhibited large differences from one region to another.

In order to see seasonal variations in vertical reflectivity structure, Fig. 5 was calculated by subtracting the JJA convective and stratiform profiles in Fig. 4 from the MAM profiles for each region. Stratiform areas in both the East Atlantic and West Africa have very stable reflectivity profiles above the  $0^{\circ}\text{C}$  level; there is no change between seasons (Figs. 5(c) and 5(d)). However, lower levels in the stratiform areas show some sensitivity to season; low-level reflectivities are 0.5–1 dB greater during JJA. Convective areas have more stable reflectivity profiles at lower levels and are more likely to vary above the  $0^{\circ}\text{C}$  level (Figs. 5(a) and 5(b)). During MAM, convective profiles are 1–3 dB greater at upper levels than during JJA over West Africa. Smaller differences occur over the East Atlantic. These comparisons suggest that reflectivity variations in stratiform areas are dominated by factors that affect the water phase (e.g. evaporation at low levels), while reflectivity variations in convective areas are dominated by factors that affect the ice phase (e.g. updraught magnitude at upper levels).

## 6. SHALLOW RAIN AND ANVIL

The Version 5 shallow isolated rain category does not represent the entire spectrum of shallow precipitating clouds. Version 6 of the 2A23 algorithm identifies an additional echo category: shallow non-isolated. Echo is labelled shallow non-isolated when it meets the shallow height criterion and is attached to echo that is not shallow. The shallow non-isolated reflectivity profiles are very similar to the shallow isolated profiles in Fig. 2(d). Together, these two shallow rain types make up the bulk of the shallow rain population highlighted by Short and Nakamura (2000), who used echo-top heights  $<3$  km to identify shallow rain. The reprocessing of Version 6 is still underway, so we used  $5^{\circ}$  resolution echo-top histograms from Version 5 TRMM product 3A25 and Short and Nakamura's 3 km height definition to identify shallow rain areal coverage.

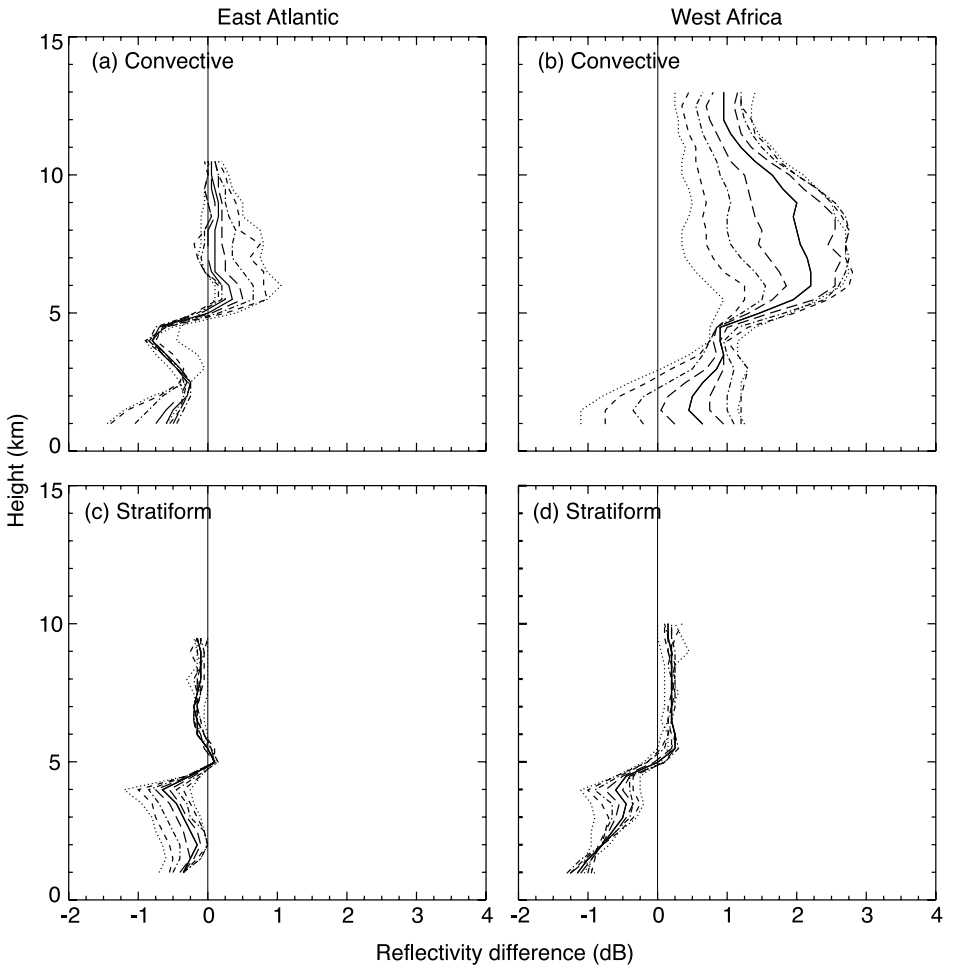


Figure 5. The MAM–JJA reflectivity profile differences in the East Atlantic and West Africa.

We chose a height of 9 km to be representative of anvil coverage using the Version 5 anvil (or ‘other’) category.

During MAM, shallow rain occurrence is prevalent over the western equatorial Atlantic and decreases rapidly eastward toward the Gulf of Guinea (Fig. 6(a)). Shallow rain covers up to 30% of the total rain area in rainy regions (cf. Figs. 6(b) and 3(a)). Very little shallow rain occurs over West Africa (less than 5% of the total rain area). The anvil area has an opposite pattern, with very little occurrence in the western Atlantic and increasing occurrence toward the East Atlantic (Fig. 6(c)). Maximum anvil coverage occurs over West Africa near the coast along the Gulf of Guinea. Anvil observable by the PR accounts for 30% of the rain area at 9 km over land and 10–15% over ocean (Fig. 6(d)). The pattern of anvil fractional coverage is very similar, but in an opposite sense, to the stratiform rain fraction map in Fig. 3(b).

During JJA, the main areas of shallow rain and anvil occurrence shift north with the rainy regions. The maximum in shallow rain area extends into the East Atlantic and more shallow rain is evident over West Africa (Fig. 6(e)). The weak maximum in anvil coverage that extended into the East Atlantic in MAM has receded (Fig. 6(g)).

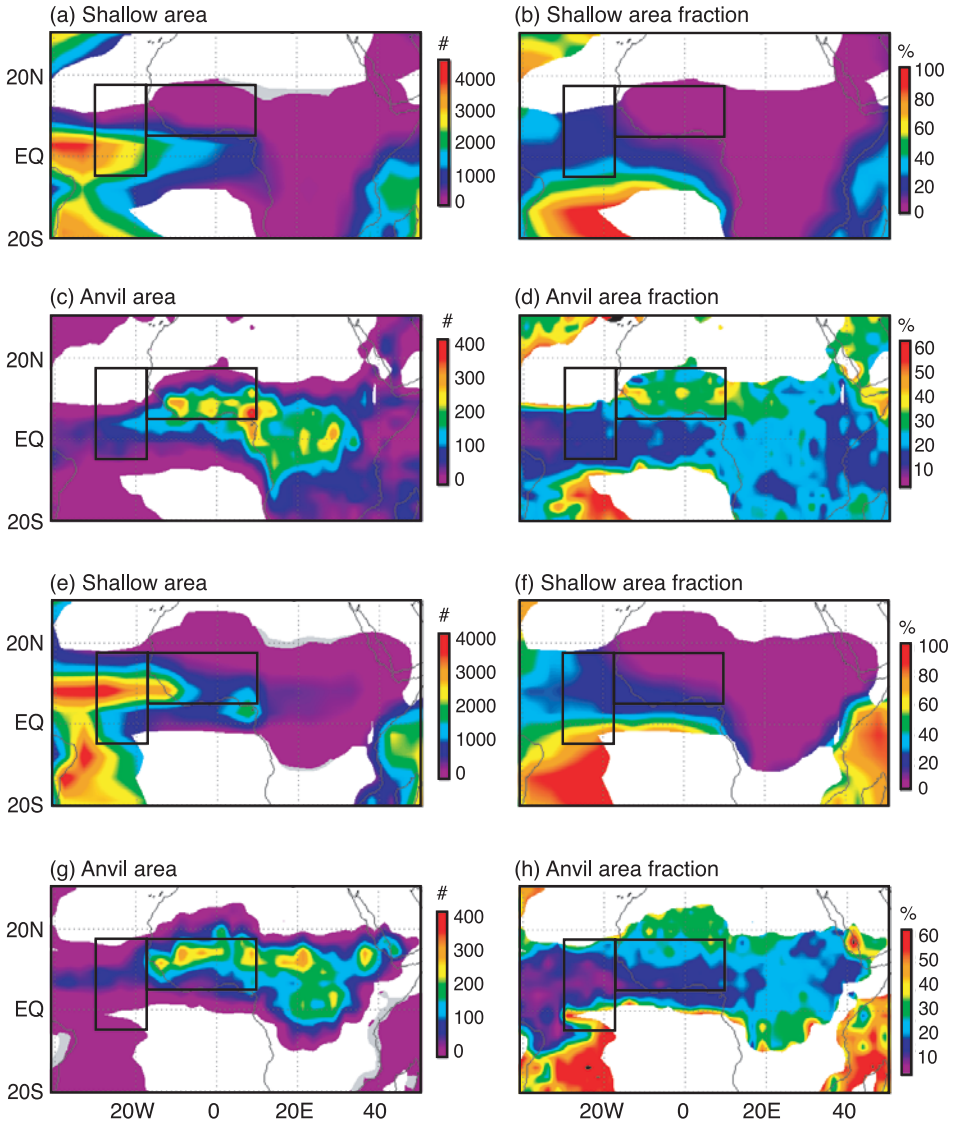


Figure 6. The average monthly count of PR observations of shallow rain (i.e. echo top <3 km) at 5° resolution and 9 km anvil at 2.5° resolution for (a–d) MAM and (e–g) JJA between 1998 and 2003. The percentage of echo area covered by shallow rain at 1.5 km and anvil at 9 km is also mapped.

The fractional rain area accounted for by shallow cells increases during JJA, especially over West Africa, while the fractional rain area covered by anvil mirrors the seasonal shift in stratiform rain fraction (Figs. 6(f) and (h)). A predominance of shallow rain and a relative lack of anvil observable by the PR appear to be indicators of regions with robust stratiform rain production.

Yuter and Houze (1998) and Houze (2004) have suggested that the large sizes attained by oceanic MCSs over the western Pacific are a result of the MCSs being in regions of high convective sustainability, i.e. located in regions where the environment, particularly the boundary layer, favours the continual formation of new convective cells

within or near an existing MCS. According to this idea, a balance is reached over time between the formation rate of new convective precipitation elements, which replenish the stratiform precipitation area, and older portions of the stratiform precipitation areas dying off. Over ocean, the sustainability of convection is supported by a warm, moist boundary layer combined with a weak diurnal cycle. These factors together favour the continual production of new convective cells. Schumacher and Houze (2003a) suggested that sustainability is limited over tropical land masses, where strong heating during the day leads to intense, short-lived convection with much less convection occurring at night. Figures 4(b) and 5(b) of Nesbitt and Zipser (2003) highlight these land/ocean diurnal variations in convective event occurrence. We suggest further that the larger population of shallow cells over ocean is likely an indicator of convective sustainability, i.e. the ability of an environment to consistently produce the moderate convection necessary for stratiform rain areas to form and mature. The anti-correlation of shallow rain to anvil area is consistent with this assessment of convective sustainability. That is, the intense, short-lived convection over land produces large ice particles (indicated by Fig. 4(b)) that fall out rapidly. Some smaller particles are left aloft, but because of the less continuous production of convective cells (indicated by a paucity of shallow convection), less material is available to form a robust stratiform area and anvil is preferentially created.

## 7. RELATIVE HUMIDITY AND WIND SHEAR

The regional environment also plays an important role in the nature of convective systems over the East Atlantic and sub-Saharan Africa. We utilize monthly NCEP reanalysis relative humidity and wind fields from 1998 to 2003 to better understand the large-scale environment's relationship to mesoscale organization and stratiform rain production. NCEP  $2.5^\circ$  values are only included in the following profiles if there is at least 50 mm average monthly rainfall in that  $2.5^\circ$  grid box.

Figures 7(a) and (b) show the NCEP relative humidity profiles for the East Atlantic and West Africa for MAM and JJA. Relative humidity is greater in JJA for both regions, especially in the midtroposphere. Because higher stratiform rain fractions occur during JJA, the profiles suggest that either a moist atmosphere assists stratiform growth or stratiform areas act to moisten the atmosphere. Humidity increases during the passage of synoptic-scale tropical easterly waves offshore from West Africa (Reed *et al.* 1977), and Cetrone and Houze (2006) found that tropical oceanic MCSs in the west Pacific occurred in environments of increased humidity and higher mid-level buoyancy associated with synoptic-scale disturbances. Sobel *et al.* (2004) and others have speculated that high relative humidity at low levels preconditions the environment for deeper convection, thus assisting stratiform rain production, while high relative humidity at upper levels results from the detrainment and evaporation of deep convective systems.

While the exact causal link between environmental relative humidity and convection remains unanswered, moister environments appear to favour convection and MCS formation and growth in several ways. Over the tropical East Atlantic, low-level relative humidity hovers around 80% and does not increase in JJA. The ocean provides an essentially infinite reservoir of low-level heat and moisture, which favours the continual generation of new cells necessary for large stratiform areas to develop and be maintained. This reservoir does not change greatly between seasons or overnight. Schumacher and Houze (2003) discussed how land versus ocean differences in stratiform rain fraction can be explained in terms of the convection being more sustainable over the ocean, where the boundary layer is warm and moist and exhibits only a weak diurnal variation.

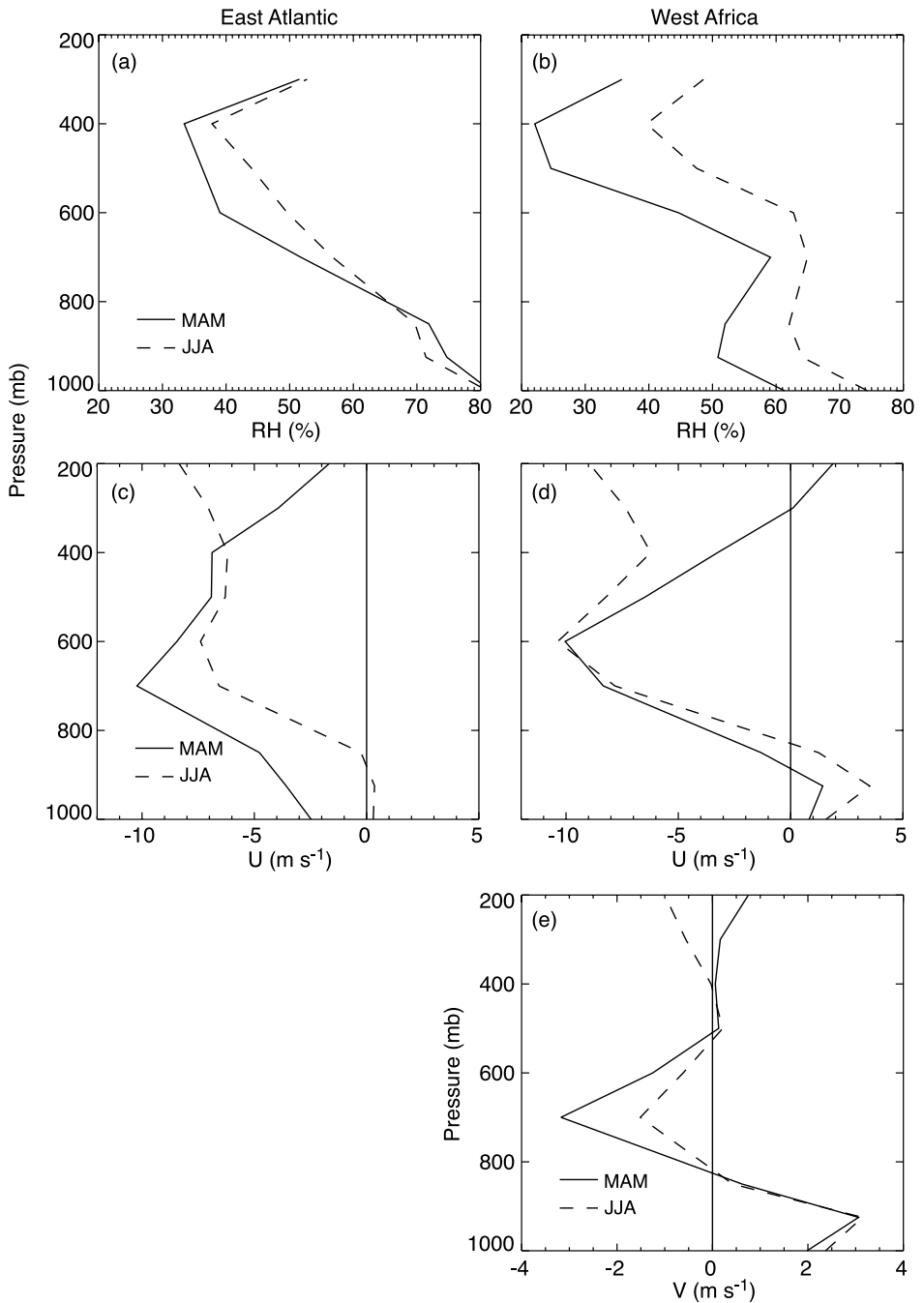


Figure 7. NCEP reanalysis average profiles over the East Atlantic and West Africa of (a–b) relative humidity, (c–d) zonal wind, and (e) meridional wind (West Africa only) for MAM and JJA between 1998 and 2003. NCEP values in a  $2.5^\circ$  grid without at least  $50 \text{ mm mo}^{-1}$  of seasonal rain were not included in the profiles.

They contrast the oceanic conditions to those over land, where despite strong surface heating during the day, the ability to support redevelopment of convection disappears at night. Over the African continent, surface heating during daytime destabilizes the low-level lapse rate and favours strong convection over land, but the stability increases at night. Thus, the continental environment does not sustain convective redevelopment around the clock. In addition, during JJA West Africa has a more maritime environment as a result of the monsoon circulation, and the near-surface relative humidity increases from 60 to over 70%. The monsoon environment with its attendant cloudiness tends to overcome diurnal controls of convective growth and dissipation related to the heating and cooling of the land surface. In addition, a more moist middle and upper troposphere will potentially decrease sublimation and evaporation within the MCS stratiform area. Thus, in the monsoon season the large-scale environment over land becomes more likely to sustain convection, thus allowing for the growth of larger MCSs and associated stratiform precipitation.

The AEJ is a zonal midtropospheric jet that is a response to the strong gradients in low-level  $\theta$  and  $\theta_e$  between the Sahara and equatorial Africa (Burpee 1972; Thorncroft and Blackburn 1999). It is most prominent at 600–700 mb over West Africa during the northern hemisphere from late spring to early autumn. The zonal wind profiles for West Africa and the East Atlantic in Figs. 7(c) and 7(d) indicate that both regions are affected by the AEJ during MAM and JJA. The strong mid-level winds of the jet may increase entrainment in stratiform clouds. Strong entrainment would increase sublimation and evaporation of the stratiform cloud mass, directly reducing stratiform rain in mesoscale regions. The AEJ is less pronounced over the East Atlantic rainy region in JJA, the season of higher stratiform rain fraction.

Strong shear exists beneath the AEJ (Burpee 1972). Rowell and Milford (1993) pointed out that squall lines preferentially occur over West Africa when low-level shear is present. In JJA, winds are more westerly at low and mid levels as a result of the south-west monsoon flow. Thus, the low-level shear remains the same or increases from MAM to JJA. Strong shear also exists above the AEJ during MAM, which is when stratiform rain fractions are lowest. We propose that upper-level shear (i.e. wind variations above 500 mb) has the potential to cause hydrometeors originating in deep convective cells to be spread beyond the stratiform rain area, resulting in less stratiform rain. The threshold value of upper-level shear that would negatively affect stratiform rain production depends on the type of convective system. Even weak shear may adversely affect stratiform rain production in situations where the convection is decaying in place. Some upper-level shear is beneficial to stratiform rain production and maintenance in leading-line/trailing stratiform systems; however, it is possible that very strong shear could also advect upper-level hydrometeors beyond the stratiform rain area in these systems.

Winds become more easterly at upper levels during JJA in association with the Tropical Easterly Jet (TEJ), a 200 mb zonal wind feature that extends from south Asia during northern hemisphere summer (Hastenrath 1991). The upper-level wind shift during JJA decreases shear substantially in both regions and occurs during the season of higher stratiform rain contributions. This reduced upper-level shear may partially explain why weak TEJs are associated with dry West African years. An increase in stratiform rain fraction is generally linked to higher rain amounts (Schumacher and Houze 2003a), and upper-level shear, if strong enough, appears to be inimical to stratiform rain production in at least some types of MCSs.

The Saharan Air Layer (SAL) is a deep layer of dry, warm air resulting from the strong heating over the Sahara Desert (Carlson and Prospero 1972). It is often evident

over West Africa in low-to-mid level northerlies that overlay near-surface southerlies (and an associated cool, moist oceanic boundary layer). The SAL can extend across the northern tropical Atlantic Ocean, but its southern boundary is generally located to the north of the main precipitation region of the East Atlantic (Karyampudi and Carlson 1988). The SAL may increase sublimation and evaporation within MCSs, thereby resulting in less stratiform rain. The meridional wind profile in Fig. 7(e) shows that West Africa is influenced by northerly flow between 850 and 500 mb. The West African relative humidity profiles in Fig. 7(b) also show a distinct kink between these heights. The decreasing northerlies at mid levels during JJA imply that the SAL is less intrusive in sub-Saharan Africa during the monsoon.

## 8. CONCLUSIONS

To summarize our regional climatology, the East Atlantic and sub-Saharan Africa receive at least  $80 \text{ mm mo}^{-1}$  of rain during MAM and JJA with the most rain occurring over West Africa during JJA (the summer monsoon). The fraction of total rain that is stratiform increases from MAM to JJA in both regions. In addition, the stratiform rain fraction is consistently higher over the East Atlantic compared to over West Africa. And while stratiform rain rates are comparable between the two regions, convective rain rates are twice as strong over West Africa. The strength of the West African convection is also indicated by the large amount of lightning that occurs over the region. Despite the fact that the convection is weaker over the East Atlantic, stratiform rain associated with organized systems such as MCSs is a large contributor to the area's rainfall. We suggest that stability and upper-level shear help explain these variations, especially in relation to stratiform rain production.

Stability variations over land versus ocean likely play an important role in convective system characteristics. Over the African continent, strong heating during the day leads to a highly unstable boundary layer and intense convection, evidenced by deep convective cells and strong convective rain rates (e.g. McGarry and Reed 1978). However, the strong diurnal cycle must also limit the lifetimes of the convective systems over land. Over the Atlantic, the sustainability of convection by a warm, moist boundary layer with a weak diurnal cycle allows the continual production of moderate convective cells, evidenced by TRMM PR observations of weaker convective rain rates and a preponderance of shallow convection. In addition, we postulate that intense but shorter-lived convection over land preferentially forms non-raining anvil (which is commonly observed by the PR over West Africa, especially in the pre-monsoon season) instead of stratiform rain since stratiform rain areas need to continually incorporate older convective material to build and sustain themselves (Houze 1997).

Upper-level wind shear can also play an important role in convective system characteristics. NCEP reanalysis fields show a decrease in upper-level shear resulting from a weaker AEJ and/or stronger TEJ during periods of higher stratiform rain fraction over the East Atlantic and sub-Saharan Africa. Houze (1993) describes the formation of stratiform rain areas in either sheared or non-sheared upper-level environments as follows. In a sheared environment (e.g. in a squall line situation), ice hydrometeors are advected from the parent convective cloud into the upper levels of the stratiform area, where the ice particles drift slowly downward while growing by diffusion in the weakly buoyant air. In a non-sheared environment, a parent convective cell may age and dissipate in place, thereby leaving ice particles aloft that can also grow by diffusion and form a stratiform area if sufficient buoyancy exists to slow the fall of the hydrometeors (Houze 1997). We suggest that if the upper-level shear is too strong, a stratiform area

will not be likely to form since the hydrometeors essential for the continued growth of a stratiform cloud will be advected too far away and anvil will preferentially form. The threshold value for when upper-level shear adversely affects stratiform rain production would be dependent on the type of convective system (e.g. the threshold will likely be higher in a leading-line/trailing stratiform system). While causality between the NCEP reanalysis shear and TRMM PR observations is not clear, it appears that a non-sheared or weakly sheared upper-level environment is more conducive to stratiform rain formation and large MCSs than a strongly sheared upper-level environment.

Further, differences in the microphysical growth of precipitation particles in the stratiform rain area do not readily explain the variations in stratiform rain contributions observed by the TRMM PR. Similar stratiform reflectivity distributions at upper levels over the East Atlantic and West Africa (and at the same location between seasons) indicate that the ice particles remaining aloft in stratiform rain areas over land are probably similar in size to (or only slightly larger than) the particles produced by oceanic convection. While the PR reflectivity profiles and TRMM lightning observations together indicate that convection over West Africa produces large ice particles (graupel) that facilitate cloud electrification, the larger ice particles produced in the intense land convection appear to fall out rapidly and not assist in the growth of stratiform rain areas. Sublimation and evaporation from higher winds and the SAL can also affect stratiform rain production by decreasing the stratiform cloud mass, but environmental stability and upper-level shear appear to be the primary factors controlling the observed variations in convective, stratiform and anvil echo areas through the production and supply of hydrometeors.

The field campaigns of GATE and COPT 81 have provided invaluable short-term observations of the convection over West Africa and the East Atlantic. The present study capitalizes on long-term satellite and reanalysis datasets to make broader statements about how the large-scale environment affects convective organization. Variations in the AEJ, TEJ, SAL and monsoon south-westerlies, and their link to stratiform rain production, may help describe the interannual variations in rainfall that dramatically affect the population of sub-Saharan Africa (Nicholson and Grist 2001). Preliminary analysis of other monsoon regions suggests that the results of this paper have wider applications: that convective sustainability and upper-level shear are essential components in determining the stratiform component of mesoscale convective systems in monsoon environments.

#### ACKNOWLEDGEMENTS

TSDIS at NASA/GSFC provided the subset orbital PR data upon which this research was based. Sean Casey and Stacy Brodzik provided invaluable computing assistance. Candace Gudmundson edited the manuscript, while Beth Tully and Kay Dewar refined the figures. This research was sponsored by NASA grant number NAG5-13654.

#### REFERENCES

- |  |      |   |
|--|------|---|
| Aspliden, C. I., Tourre, Y. and Sabine, J. B.      | 1976 | Some climatological aspects of West African disturbance lines during GATE. <i>Mon. Weather Rev.</i> , <b>104</b> , 1029–1035  |
| Awaka, J., Iguchi, T., Kumagai, H. and Okamoto, K. | 1997 | 'Rain type classification algorithm for TRMM Precipitation Radar'. Pp. 1633–1635 in Proc. of the IEEE 1997 International Geoscience and Remote Sensing Symposium, August 3–8, Singapore |

- Biggerstaff, M. I. and Houze, R. A., Jr. 1993 Kinematics and microphysics of the transition zone of the 10–11 June 1985 squall line. *J. Atmos. Sci.*, **50**, 3091–3110
- Boccippio, D. J., Goodman, S. J. and Heckman, S. 2000 Regional differences in tropical lightning distributions. *J. Appl. Meteorol.*, **39**, 2231–2248
- Bolen, S. M. and Chandrasekar, V. 2000 Quantitative cross validation of space-based and ground-based radar observations. *J. Appl. Meteorol.*, **39**, 2071–2079
- Burpee, R. W. 1972 The origin and structure of easterly waves in the lower troposphere of North Africa. *J. Atmos. Sci.*, **29**, 77–90
- Carlson, T. N. 1969a Synoptic histories of three African disturbances that developed into Atlantic hurricanes. *Mon. Weather Rev.*, **97**, 256–276
- 1969b Some remarks on African disturbances and their progress over the tropical Atlantic. *Mon. Weather Rev.*, **97**, 716–726
- Carlson, T. N. and Prospero, J. M. 1972 The large-scale movement of Saharan air outbreaks over the northern equatorial Atlantic. *J. Appl. Meteorol.*, **11**, 283–297
- Cetrone, J. and Houze, R. A., Jr. 2006 Characteristics of tropical convection over the ocean near Kwajalein. *Mon. Weather Rev.*, **134**, 834–853
- Chong, M. and Hauser, D. 1989 A tropical squall line observed during the COPT 81 experiment in West Africa. Part II: Water budget. *Mon. Weather Rev.*, **117**, 728–744
- Chong, M., Amayenc, P., Scialom, G. and Testud, J. 1987 A tropical squall line observed during the COPT 81 experiment in West Africa. Part I: Kinematic structure inferred from dual-Doppler radar data. *Mon. Weather Rev.*, **115**, 670–694
- Cook, K. H. 1999 Generation of the African easterly jet and its role in determining West African precipitation. *J. Climate*, **12**, 1165–1184
- Diedhiou, A., Janicot, S., Viltard, A., de Felice, P. and Laurent, H. 1999 Easterly wave regimes and associated convection over West Africa and tropical Atlantic: Results from the NCEP/NCAR and ECMWF reanalyses. *Climate Dynamics*, **15**, 795–822
- Eldridge, R. H. 1957 A synoptic study of west African disturbance lines. *Q. J. R. Meteorol. Soc.*, **83**, 303–314
- Fortune, M. 1980 Properties of African squall lines inferred from time-lapse satellite imagery. *Mon. Weather Rev.*, **108**, 153–168
- Geerts, B. and Dejene, T. 2005 Regional and diurnal variability of the vertical structure of precipitation systems in Africa based on spaceborne radar data. *J. Climate*, **18**, 893–916
- Grist, J. P. and Nicholson, S. E. 2001 A study of the dynamic factors influencing the rainfall variability in the West African Sahel. *J. Climate*, **14**, 1337–1359
- Hamilton, R. A. and Archbold, J. W. 1945 Meteorology of Nigeria and adjacent territory. *Q. J. R. Meteorol. Soc.*, **71**, 231–264
- Hastenrath, S. 1991 *Climate dynamics of the tropics*. Kluwer Academic Publishers
- Hirose, M. and Nakamura, K. 2004 Spatiotemporal variation of the vertical gradient of rainfall rate observed by the TRMM precipitation radar. *J. Climate*, **17**, 3378–3397
- Hodges, K. I. and Thorncroft, C. D. 1997 Distribution and statistics of African mesoscale convective weather systems based on the ISCCP Meteosat imagery. *Mon. Weather Rev.*, **125**, 2821–2837
- Houze, R. A., Jr. 1977 Structure and dynamics of a tropical squall-line system. *Mon. Weather Rev.*, **105**, 1540–1567
- 1989 Observed structure of mesoscale convective systems and implications for large-scale heating. *Q. J. R. Meteorol. Soc.*, **115**, 425–461
- 1993 *Cloud dynamics*. Academic Press
- 1997 Stratiform precipitation in regions of convection: A meteorological paradox? *Bull. Am. Meteorol. Soc.*, **78**, 2179–2196
- 2004 Mesoscale convective systems. *Rev. Geophys.*, **42**, RG4003, doi: 10.1029/2004RG000150
- Houze, R. A., Jr. and Betts, A. K. 1981 Convection in GATE. *Rev. Geophys. Space Phys.*, **19**, 541–576
- Houze, R. A., Jr. and Cheng, C.-P. 1977 Radar characteristics of tropical convection observed during GATE: Mean properties and trends over the summer season. *Mon. Weather Rev.*, **105**, 964–980
- Iguchi, T., Kozu, T., Meneghini, R., Awaka, J. and Okamoto, K. 2000 Rain-profiling algorithm for the TRMM Precipitation Radar. *J. Appl. Meteorol.*, **39**, 2038–2052
- Karyampudi, V. M. and Carlson, T. N. 1988 Analysis of numerical simulations of the Saharan air layer and its effect on easterly wave disturbances. *J. Atmos. Sci.*, **45**, 3102–3136

- Kozu, T., Kawanishi, T., Kuroiwa, H., Kojima, M., Oikawa, K., Kumagai, H., Okamoto, K., Okumura, M., Nakatsuka, H. and Nishikawa, K. 2001 Development of precipitation radar onboard the Tropical Rainfall Measuring Mission (TRMM) satellite. *IEEE Trans. Geosci. Remote Sensing*, **39**, 102–116
- Kummerow, C., Barnes, W., Kozu, T., Shiue, J. and Simpson, J. 1998 The Tropical Rainfall Measuring Mission (TRMM) sensor package. *J. Atmos. Oceanic Technol.*, **15**, 809–817
- Laing, A. G. and Fritsch, J. M. 1993 Mesoscale convective complexes in Africa. *Mon. Weather Rev.*, **121**, 2254–2263
- Landsea, C. W. and Gray, W. M. 1992 The strong association between western Sahelian monsoon rainfall and intense Atlantic hurricanes. *J. Climate*, **5**, 435–453
- Leary, C. A. and Houze, R. A., Jr. 1979 The structure and evolution of convection in a tropical cloud cluster. *J. Atmos. Sci.*, **36**, 437–457
- Lebel, T., Diedhiou, A. and Laurent, H. 2003 Seasonal cycle and interannual variability of the Sahelian rainfall at hydrological scales. *J. Geophys. Res.*, **108**, 8389, doi: 10.1029/2001JD001580
- McGarry, M. M. and Reed, R. J. 1978 Diurnal variations in convective activity and precipitation during Phases II and III of GATE. *Mon. Weather Rev.*, **106**, 101–113
- Maddox, R. A. 1980 Mesoscale convective complexes. *Bull. Am. Meteorol. Soc.*, **61**, 1374–1387
- Martin, D. W. and Schreiner, A. J. 1981 Characteristics of West African and East Atlantic cloud clusters: A survey from GATE. *Mon. Weather Rev.*, **109**, 1671–1688
- Mohr, K. I., Famiglietti, J. S. and Zipser, E. J. 1999 The contribution to tropical rainfall with respect to convective system type, size, and intensity estimated from the 85-GHz ice-scattering signature. *J. Appl. Meteorol.*, **38**, 596–606
- Nesbitt, S. W. and Zipser, E. J. 2003 The diurnal cycle of rainfall and convective intensity according to three years of TRMM measurements. *J. Climate*, **16**, 1456–1475
- Nicholson, S. E. and Grist, J. P. 2001 A conceptual model for understanding rainfall variability in the West African Sahel on interannual and interdecadal timescales. *Int. J. Climatol.*, **21**, 1733–1757
- Payne, S. W. and McGarry, M. M. 1977 The relationship of satellite inferred convective activity to easterly waves over West Africa and adjacent ocean during Phase III of GATE. *Mon. Weather Rev.*, **105**, 413–420
- Reed, R. J., Norquist, D. C. and Recker, E. E. 1977 The structure and properties of African wave disturbances as observed during Phase III of GATE. *Mon. Weather Rev.*, **105**, 317–333
- Roux, F. 1988 The West African squall line observed on 23 June 1981 during COPT 81: Kinematics and thermodynamics of the convective region. *J. Atmos. Sci.*, **45**, 406–426
- Rowell, D. P. and Milford, J. R. 1993 On the generation of African squall lines. *J. Climate*, **6**, 1181–1193
- Schumacher, C. and Houze, R. A., Jr. 2000 Comparison of radar data from the TRMM satellite and Kwajalein oceanic validation site. *J. Appl. Meteorol.*, **39**, 2151–2164
- 2003a Stratiform rain in the tropics as seen by the TRMM Precipitation Radar. *J. Climate*, **16**, 1739–1756
- 2003b The TRMM Precipitation Radar's view of shallow, isolated rain. *J. Appl. Meteorol.*, **42**, 1519–1524
- Sealy, A., Jenkins, G. S. and Walford, S. C. 2003 Seasonal/regional comparisons of rain rates and rain characteristics in West Africa using TRMM observations. *J. Geophys. Res.*, **108**, 4306, doi: 10.1029/2002JD002667
- Shimizu, S., Takahashi, N., Iguchi, T., Awaka, J., Kozu, T., Meneghini, R. and Okamoto, K. 2003 'Validation analyses after the altitude change of TRMM'. Pp. 83–91 in *Microwave Remote Sensing of the Atmosphere and Environment III*. Eds. C. D. Kummerow, J. S. Jiang and S. Uratuka. Proceedings of the SPIE, Vol. 4894
- Short, D. A. and Nakamura, K. 2000 TRMM radar observations of shallow precipitation over the tropical oceans. *J. Climate*, **13**, 4107–4124
- Sobel, A. H., Yuter, S. E., Bretherton, C. S. and Kiladis, G. N. 2004 Large-scale meteorology and deep convection during TRMM KWAJEX. *Mon. Weather Rev.*, **132**, 422–444
- Sommeria, G. and Testud, J. 1984 COPT 81: A field experiment designed for the study of dynamics and electrical activity of deep convection in continental tropical regions. *Bull. Am. Meteorol. Soc.*, **65**, 4–10
- Thorncroft, C. D. and Blackburn, M. 1999 Maintenance of the African easterly jet. *Q. J. R. Meteorol. Soc.*, **125**, 763–786

- Thorncroft, C. and Hodges, K. 2001 African easterly wave variability and its relationship to Atlantic tropical cyclone activity. *J. Climate*, **14**, 1166–1179
- Toracinta, E. R. and Zipser, E. J. 2001 Lightning and SSM/I-ice-scattering mesoscale convective systems in the global tropics. *J. Appl. Meteorol.*, **40**, 983–1002
- Yang, G.-Y. and Slingo, J. 2001 The diurnal cycle in the tropics. *Mon. Weather Rev.*, **129**, 784–801
- Yuter, S. E. and Houze, R. A., Jr. 1998 The natural variability of precipitating clouds over the western Pacific warm pool. *Q. J. R. Meteorol. Soc.*, **124**, 53–99
- Zipser, E. J. 1969 The role of organized unsaturated convective downdrafts in the structure and rapid decay of an equatorial disturbance. *J. Appl. Meteorol.*, **8**, 799–814
- 1977 Mesoscale and convective-scale downdrafts as distinct components of squall-line structure. *Mon. Weather Rev.*, **105**, 1568–1589